# Development of a Corrosion Inhibitor for the Closed-Loop Cooling Water System of Blast Furnace

**HSIN-HUNG OU**

*New Materials Research & Development Department*
*China Steel Corporation*

A new corrosion inhibitor (ECOSW) has been developed for the closed-loop cooling water system of blast furnace. Instead of using a commercial corrosion inhibitor (CPSW), which mainly contains molybdate and nitrite, ECOSW consists of gluconate along with a relatively low amount of molybdate. The laboratory-level assessments of corrosion inhibition for carbon steel (C-steel) including weight loss measurement and electrochemical analysis reveal that the corrosion of C-steel in the presence of ECOSW is thermodynamically and kinetically unfavorable as compared to that with CPSW. According to the investigations based on SEM/FIB, FTIR, and XPS, an inhibition mechanism was proposed whereby the gluconate could bridge the molybdate and iron, which is responsible for the formation of the protective film. Pilot testing over a one month span showed that the corrosion rates of C-steel coupons in the presence of ECOSW and CPSW were 0.065 and 0.11 MPY, respectively. The microbial population in the presence of ECOSW was one order of magnitude higher than that of CPSW, but was still lower than the maximum acceptable level by two orders of magnitude.

Keywords: Corrosion inhibitor, Closed-loop, Cooling water system

## 1. INTRODUCTION

There are three types of industrial cooling water systems including once-through, open recirculating, and closed recirculating or closed loops[1]. In the case of once- through system, the intake water is typically supplied from seawater, lake water, river water, and etc., which passes through the heat exchanger only once and then discharges the water back to the same source, but in a different location to prevent recycling (e.g., no recirculation occurs). On the other hand, the water in an open circulating system is heated in the heat exchanger and then releases the heat at a cooling tower. Continuous make-up water is necessary as this type of water system may lose water consistently owing to evaporation and wind drift. Moreover, intermittent blow-downs are important as an excessive level of minerals could lead to a scaling problem. In terms of the closed-loop cooling water system, heat produced during the manufacturing process is transferred to the closed cooling water loop by heat exchange equipment and removed from the closed system loop by a second heat exchanger. In other words, the same water is used all the time in a closed loop with negligible loss to the atmosphere. Technically, with the closed-loop cooling water system it is easier to secure the water quality compared to the other systems as there is little chance of cross contamination between closed-loop water and surrounding environment. Corrosion and microorganism growth are two issues in a closed-loop cooling water system whereas scaling problem is generally not a concern. However, such a system must be handled with a great care because any unexpected failure may lead to a leak of cooling water into the high temperature reactor with possibly catastrophic consequences.

As far as the corrosion issue is concerned, molybdate has become a common and popular corrosion inhibitor in closed-loop water systems since the use of chromate-based inhibitors was banned under environmental regulations[2]. Despite its many similarities to chromate, the oxidation capability of molybdate is not as excellent as chromate and only in the presence of a primary passivator can they inhibit corrosion as anodic inhibitors. Therefore, the combined use of molybdate with synergistic constituents in formulations appears to be a reasonable approach for obtaining sufficient efficiency to replace chromate inhibition. For example, the inhibition efficiency can be significantly improved when nitrite is used along with molybdate[3]. In spite of the considerable use of molybdenum in industry, no incidences have yet been reported of industrial poisoning by molydenum. Molybdate seems to be free of any accompanying toxic elements or compounds, and exhibits an environmental compatibility within the

framework of its commercial utilization as a corrosion inhibitor. However, the price of molybdenum fluctuates significantly depending on market conditions. The development of an inhibitor formulation with relatively low amount of molybdenum appears to be of great urgency in consideration of cost management. In this regard, gluconate has been reported to be an alternative corrosion inhibitor as it is environmentally friendly with cost and performance effectiveness[4,5]. Gluconate has also been considered an excellent material to inhibit the chloride pitting corrosion[6]. In this study, a competitive formulation of corrosion inhibitor was developed for the closed-loop cooling water system. The inhibition performance was examined using weight-loss measurement and electrochemical analysis. A suggested mechanism was also proposed according to the results obtained from SEM/FIB, FTIR and XPS. In addition, a complementary biocide program was created to suppress the possible bacterial growth.

## 2. EXPERIMENTAL METHODS

### 2.1 Evaluation of performance of corrosion inhibitor

The methods we used to evaluate the performance of the developed corrosion inhibitors include weight-loss measurement, potentiodynamic polarization and pilot test. The apparatus for the weight-loss measurement was modified from jar-testing equipment (Fig.1) in which the nitrogen purge tube and hotplate are equipped to adjust the concentration of dissolved oxygen and the temperature in the test solution. The test coupons were prepared by polishing with 240-grit papers and then cleaned with a homemade cleaning reagent before being weighted by an electronic balance with a sensitivity of 0.1 mg. The pretreated coupons were subsequently fixed on paddle stirrers with specific acrylic clamps. Prior to the tests, the solutions were stirred at 100 rpm for 30 min in order to achieve the formation of homogeneous dense films on the coupons. The efficiency of corrosion inhibition was calculated by weighing the coupons before and after the tests. The weight-loss experiments were performed in triplicate. The performance of two inhibitors by the names of ECOSW and CPSW were comparatively evaluated, which are our developed corrosion inhibitor and the commercial product provided by the water treatment engineers in the blast furnace, respectively.

The electrochemical analysis was performed using a conventional three-electrode cell assembly. The cell consists of a Pt electrode and a $Hg/HgCl_2$ electrode as counter and reference electrode, respectively. The C-steel electrode with an exposed area of 1 $cm^2$ was used as a working electrode. All the tests were performed under an unstirred condition with no aeration. The working electrode was immersed for 60 min before the start of scan to attain a stable state. The polarization studies were carried out over a potential of 0 to -1 V span versus open circuit potential at a scan rate of 0.5 $mVs^{-1}$.
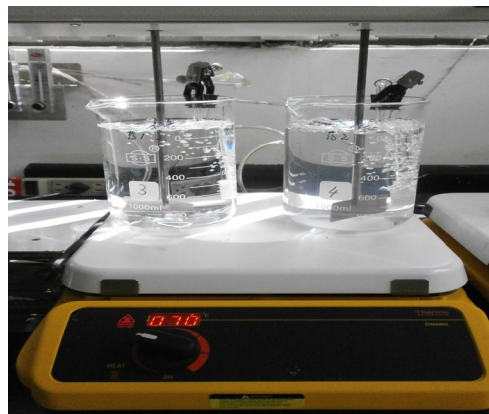


**Fig.1.** Laboratory scale apparatus with supporting devices to simulate the water quality in the field (The concentration of dissolved oxygen in the closed-loop cooling water system of blast furnace is around 4 ppm and the water temperature rises up to 60 $^oC$ periodically).

### 2.2 Determination of bacterial population

The number of microorganism was roughly determined by comparing the density of the colonies appearing on the slide with densities shown on a model chart provided by Merck. The incubation time and temperature are 48 h and 30$^oC$, respectively.

### 2.3 Characterization of C-steel after immersed in CPSW and ECOSW

FTIR spectra of the C-steel coupons after immersion in the inhibitors were performed in the transmission mode ranging from 400 to 4000 $cm^{-1}$ with a resolution of 2 $cm^{-1}$ and accumulation of 128 scans. The specimen for FTIR characterization was assumed to be the complex film formed on the C-steel surface after immersion for 24 h in 0.5N HCl. SEM was employed to observe the surface morphology of C-steel with and without the presence of the inhibitor in an acidic medium. The images were taken after immersing the samples for 24 h in 0.5N HCl with and without the corrosion inhibitor. XPS measurements were performed with X-ray radiation and monochromatic. High resolution scans with 0.1 eV step was conducted over the regions of interest including Fe 2p, O1s, N1s and C1s. Broad scan spectra were obtained with pass energy of 150 eV, while narrow scans of Fe 2p, O1s, N1s and C1s used a pass energy of 15 eV. All XPS spectra were referenced to the Fe $2p^{3/2}$ line of C-steel coupon (710.6 eV) without the presence of inhibitor.

## 3. RESULTS AND DISCUSSION

### 3.1 Weight loss measurement

The corrosion rates of C-steel coupons with and without the presence of ECOSW and CPSW are listed in Table 1. Both ECOSW and CPSW exhibit excellent inhibiting effects upon the C-steel coupons. We observed no significant difference in the capability of corrosion inhibition between ECOSW and CPSW. On the other hand, it is noteworthy that the concentrations of molybdate and nitrite of ECOSW are one-fifth and half of that of CPSW, respectively. It appears that gluconate successfully replaces molybdate or considerably reduces the required amount of molybdate for suppressing the corrosion of C-steel. In other words, ECOSW achieved a similar performance as a commercial product (i.e., CPSW) in corrosion inhibition of C-steel at only half the price of CPSW.

### 3.2 Control of microorganism growth

Bacterial growth may be a big issue when ECOSW is used in the water system because gluconate is an ideal nutritional supplement for bacterial growth. Despite microorganisms likely contribute corrosion inhibition by neutralizing the corrosive substances, forming a protective film, and stabilizing a pre-existing protective film on a metal, the colonization of bacteria on a metal surface also favors corrosive reactions through the stimulation of the anodic reaction by acidic metabolites or the cathodic reaction by microbial production of new alternative carhodic reactant (e.g., $H_2S$) [7]. In spite of the debate over the microorganism issue, the effect of the bacterial growth on the C-steel corrosion is especially in the focus of research interest.

In order to prevent or reduce biocorrosion, the selection of biocides and the design of technological equipment, as well as the proper and regular cleaning of the equipment, are of extreme importance. In our research, determination kits for microorganism population were used to examine the control efficiency of bacterial growth by biocide programs. Figure 2 shows the bacterial population over time in the presence of CPSW and ECOSW as a function of biocide program. As shown in Fig.2, leaving program 1 (CPSW) out of consideration, negligible bacterial populations were observed at the end of first two weeks in the cases of

**Table 1** Corrosion rates, corrosion potentials, corrosion currents, and of C-steel coupons without and with the presence of corrosion inhibitors

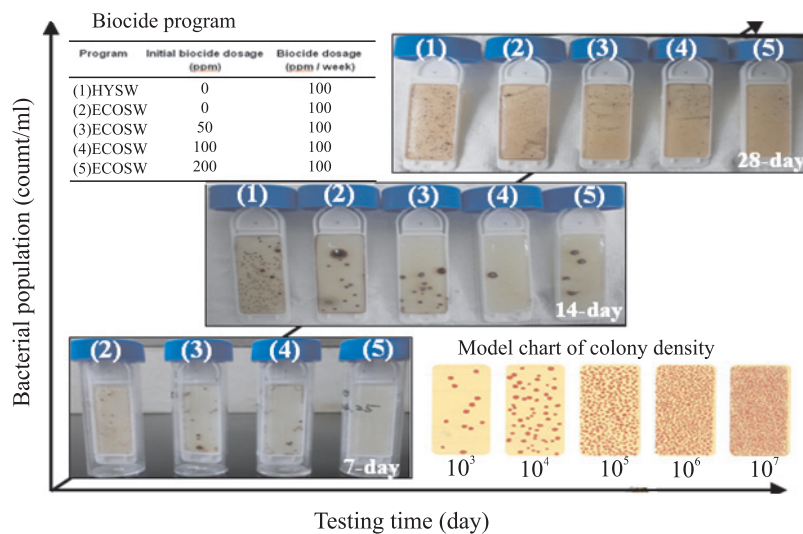| Sample | Corrosion rate (MPY) | Corrosion potential (mV vs Hg/HgCl$_2$) | Corrosion current (mA/cm$^2$) |
|---|---|---|---|
| Blank | 22.4 | -616 | 1.81E-4 |
| ECOSW | 0.009~0.049 | -473 | 1.91E-5 |
| CPSW | 0.007~0.053 | -494 | 3.91E-5 |



**Fig.2.** Bacterial populations in the cases of ECOSW and CPSW over time as functions of different biocide programs.

ECOSW with different biocide programs. Further extension of duration to 28 days led to increases in the number of microorganisms, with the level of bacterial populations reaching $10^3 \sim 10^4$ count/ml (the control value of bacterial population in practice is $10^5$ count/ml). On the other hand, the corrosion rates of C-steel coupons with 1~5 biocide programs were 0.12, 2.54, 0.07, 0.11 and 0.08 MPY, respectively. This result grantees that ECOSW along with a complementary and appropriate biocide program offer a solution to possible corrosion and bacterial growth problems.

### 3.3 Polarization studies

Figure 3 shows the polarization curves of C-steel coupons at 25°C after 1h immersion in the absence of and in the presence of CPSW and ECOSW. In an attempt to simulate the water quality of closed-loop cooling water system of blast furnace, the electrolyte for electrochemical analysis contained 100 ppm $Cl^{-1}$ and 50 ppm Ca-H with pH approximately at 9.5. Electrochemical parameters including corrosion potential ($E_{corr}$), and corrosion current ($I_{corr}$) are demonstrated in Table 1. Compared to the case without the presence of inhibitor, the positive shift of $E_{corr}$ and the decrease in $I_{corr}$ in both cases of CPSW and ECOSW are not only indicative of an effective corrosion inhibition of C-steel, but also suggests that either CPSW or ECOSW inhibitor acts as anodic inhibitor. A further examination of $E_{corr}$ and $I_{corr}$ reveals that the corrosion of a C-steel coupon in the presence of ECOSW is thermodynamically and kinetically unfavorable as compared to that with CPSW.
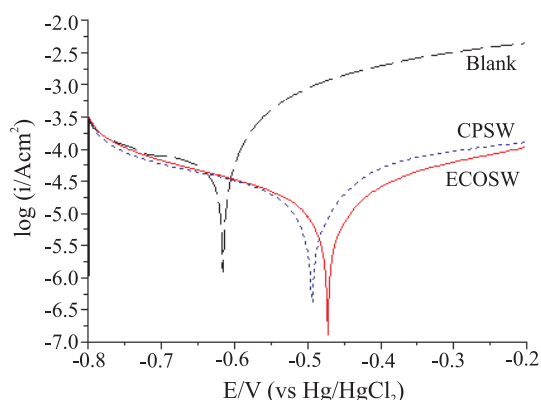


**Fig.3.** Polarization curves of C-steel immersed in the corrosive solutions (0.2N HCl) without and with the presence of ECOSW and CPSW.

Further investigation of the cathodic current density reveals that the cathodic polarization curves in the presence of inhibitors are slightly shifted towards a lower current density side which is attributable to the suppression of cathodic reactions. In other words, the decrease of $H^+$ ions on the surface of C-steel took place mainly through a charge transfer mechanism as the cathode hydrogen evolution in the presence of either CPSW or ECOSW was not significantly modified. This observation corresponds to the fact that the decrease in the $I_{corr}$ value is due to the weaker retardation of cathodic reaction as compared with the corresponding anodic one. On the other hand, in the anodic part of polarization, the anodic current densities of both ECOSW and CPSW are lower than that of blank one. This phenomenon can be explained on the basis that both inhibitors are adsorbed on the anodic sites of the C-steel coupon and thereby decrease the dissolution of metallic iron. Moreover, the relatively low anodic current density in the case of ECOSW compared to CPSW indicates that the adsorption of ECOSW over a C-steel surface is more efficient than CPSW.

### 3.4 SEM

The surface morphologies of C-steel coupons before and after immersion in the corrosion inhibitors are shown in Fig.4. The coupon surface was severely destroyed where the morphology was rough, bumpy and uneven when no corrosion inhibitor was present in the corrosive medium (Fig.4a). In comparison, the surface morphology of coupon in the presence of either ECOSW (Fig.4b) or CPSW (Fig.4c) showed the longitudinal and parallel grinding grooves which was as the same as the bare coupon shown in the insert of Fig.4b. This result indicates a successful protection of the C-steel coupons from corrosion, which is possibly attributable to the formation of a protective film.

Further investigation was also conducted by cross-sectional observation using SEM-FIB. Figure 4d shows the cross-sectional view of a coupon in the absence of inhibitor with only two layers being observable which corresponding to the carbon-coating layer and underneath substrate, respectively In comparison, in Figs.4e and 4f, illustrating the cross-sectional view of a coupon in the presence of either ECOSW or CPSW, a smooth protective layer is clearly observed between the carbon-coating layer and the substrate. The layer thicknesses were measured approximately at 900 and 800 nm for ECOSW and CPSW, respectively. These images provide solid evidence for the formation of a protective film, which accounts for the protection of C-steel from corrosion. One interesting point is that the thickness of this protective film is thicker with ECOSW than with CPSW, which may partly reveal that the efficiency of inhibition is film thickness-dependent.
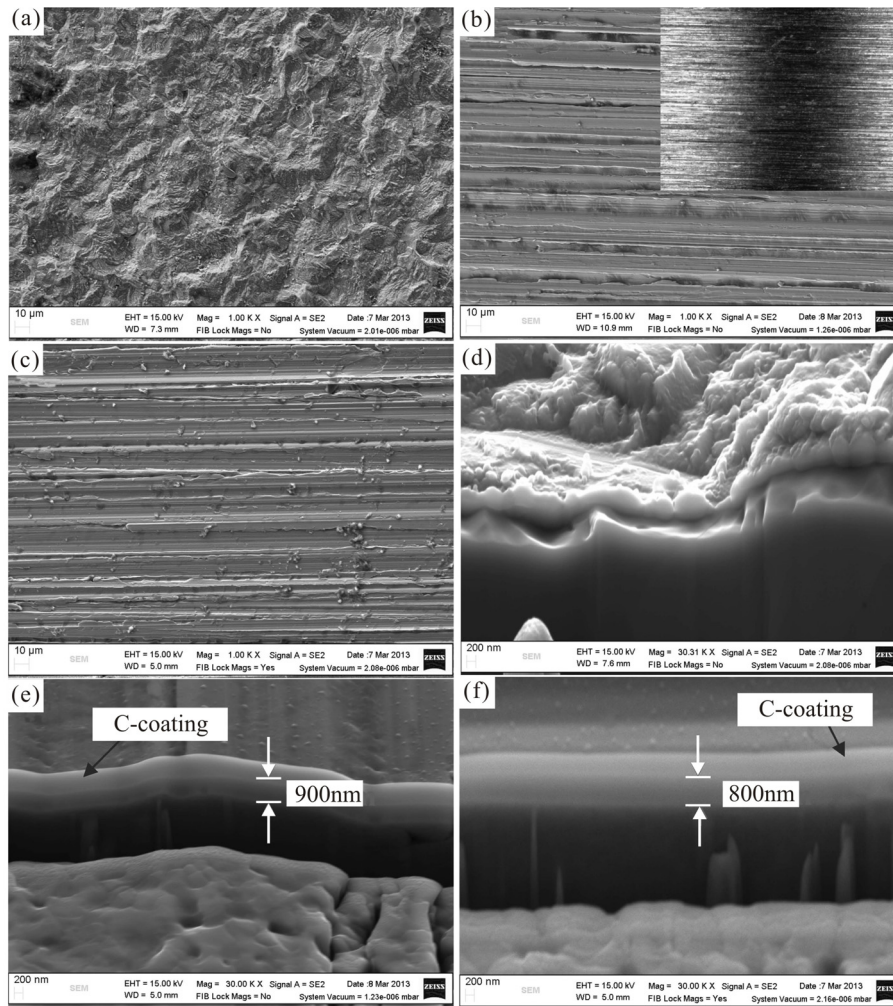
**Fig.4.** Surface morphologies of C-steel coupons (a) without and with the presence of (b) ECOSW and (c) CPSW inhibitors; Cross-sectional views of C-steel (d) without and with the presence of (e) ECOSW and (f) CPSW inhibitors.

### 3.5 FTIR

FTIR examinations were also carried out to investigate the possible adsorption mechanism over the C-steel surface. As shown in Fig.5, the IR spectrum of a C-steel coupon after immersion in a corrosive medium containing ECOSW reveals the adsorption of gluconate, molybdate and nitrite over the C-steel surface. Two diagnostic vibrations for nitrite show up at 1244 and 1730 $cm^{-1}$ whereas another characteristic vibration at 810 $cm^{-1}$ is obscure. Two weak, but still clear and identifiable, vibrations or stretchings at 840 and 2912 $cm^{-1}$ for molybdate were observed in the case of ECOSW. In terms of the footprints of gluconate, the peaks showing at 1600 $cm^{-1}$ can be attributed to the vibrations of $C = O$ of gluconate but the broad OH stretch obscures the CH region around 3000~3400 $cm^{-1}$. Other vibrations and stretching of gluconate are intense which indicates the strong adsorption of gluconate over the C-steel surface.
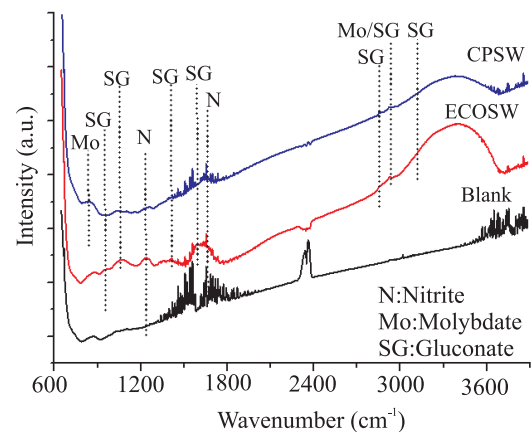


**Fig.5.** FTIR spectra of C-steel coupons before and after immersion in the corrosive solutions (0.2N) containing ECOSW and CPSW.

In comparison, the peaks attributed to molybdate and nitrite were also observed in the case of CPSW but the intensities are relatively weak. The relatively strong peak intensity in the case of ECOSW can be possibly explained by the fact that more nitrite and molybdate adsorb on the C-steel surface through the chelating property of gluconate that bridges the iron surface and molybdate/nitrite. Furthermore, the shifts of vibrations in the case of ECOSW to the higher wavenumber were observed as compared to CPSW, which is likely as a result of the participation of gluconate between C-steel surface and molybdate/nitrite binding.

### 3.6 XPS

Deconvolutions of Fe $2p^{2/3}$ spectra for the C-steel coupons after immersion in the ECOSW and HYSM inhibitors are shown in Figs.6a and 6b, respectively. In the case of CPSW, a characteristic peak shows at 707.1 eV along with another one appearing at 709.6 eV.

The former peak is attributable to the metallic metal while the latter one is probably due to ferric compounds, such as $Fe_2O_3$, $FeOOH$ and $FeCl_3$. In comparison, the Fe $2p^{3/2}$ spectrum shown in Fig.6a for ECOSW shows one exclusive peak at 707.8 eV in addition to the peaks at 706.9 eV (metallic iron) and 710.1 eV (ferric compound). The peak appearing at 707.8 eV can be ascribed to the ferrous compound which is likely as a result of chelation between gluconate and C-steel. This result is consistent with the conclusion obtained from FTIR analysis in that the presence of gluconate is in favor of the formation of a complex compound which is responsible for the protection of C-steel from corrosion.

Further evidence is also available in terms of O1s spectra (Figs.6c and 6d). Upon deconvoluting O1s spectrum in the case of HYSE, three peaks are in sharp at 530.3, 531.4 and 532.5 eV which are assigned to the oxygen bonded to $Fe^{3+}$ ($Fe_2O_3$, $Fe_3O_2$ and $FeO$), oxygen in hydrous iron oxides ($FeOOH$ or $Fe(OH)_3$) and
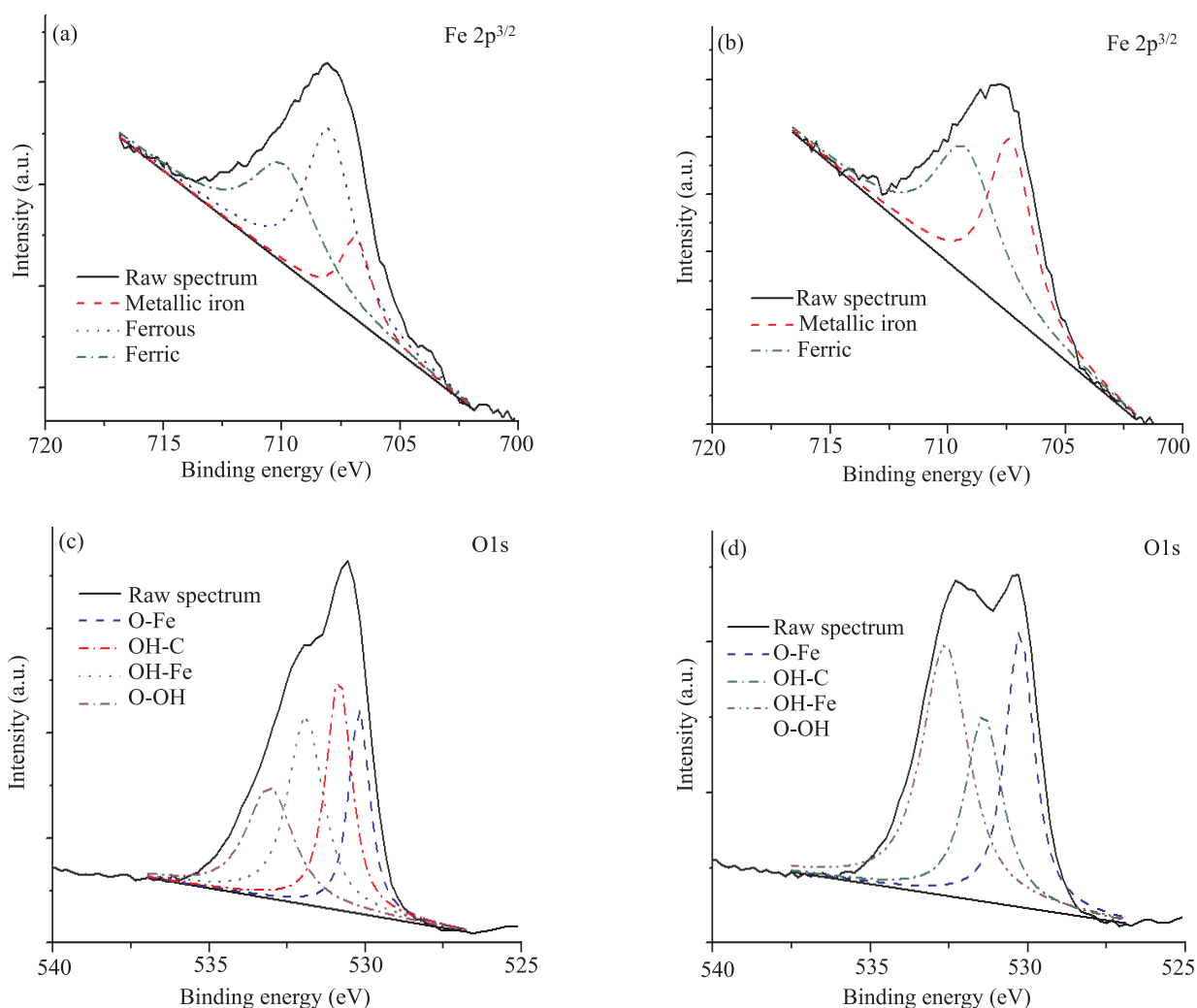


**Fig.6.** Fe $2p^{3/2}$ and O1s spectra of C-steel coupons after immersion in the corrosive solutions (0.2N) containing (a, c) ECOSW and (b, d) CPSW.

oxygen of adsorbed water ($H_2O$), respectively[8]. In comparison, in addition to the same peaks in CPSW, an additional peak spiking at 530.9 eV in the case of ECOSW is attributable to the oxygen in hydroxyl or carboxyl group of gluconate. This result corresponds to the fact that gluconate is strongly bonded to the C-steel surface. In addition, the oxygen ratio in favor of O-Fe is also evidence of the strong involvement of gluconate in the corrosion inhibition. A suggested mechanism is proposed below based on the coupled results from SEM, FTIR and XPS. In general, the primary mechanism of corrosion inhibition is owing to the formation of $\gamma$–$Fe_2O_3$ at the anodic sites as a result of thermodynamically favorable reaction from Fe(0) to Fe(III). In case the corrosion inhibitor is involved in the corrosive medium, it would adsorb over metallic iron surface or incorporate into $\gamma$–$Fe_2O_3$ which suppresses the $Fe^{2+}$ release or repairs the attacked spots in $\gamma$–$Fe_2O_3$[9]. Our proposed mechanism suggests that the adsorption of gluconate over the C-steel surface is a prerequisite for the binding between d-orbital of iron atoms, involving the displacement of water molecules from the metallic Fe surface, and the lonely $sp^2$ electron pairs present in the O atoms of gluconate. Oxygen bridged complexes with Fe(II) substrate are likely to be responsible for the formation of a protective layer. The generated layer blocks the competitive adsorption of aggressive anions such as chloride and sulfate ions, resulting in the corrosion inhibition of metallic iron. On the other hand, the incorporation of gluconate into $\gamma$–$Fe_2O_3$ film is also possible as evidenced by XPS analysis. Gluconate may act as a stabilizer through its incorporation into the $\gamma$–$Fe_2O_3$ film and repair the inhomogeneous porous oxide layer. As soon as the sparingly-soluble complexes are formed at anodic sites, the relative bond strength of iron ion with the lattice oxygen of $Fe_2O_3$ and with the gluconate will be of utmost importance, which accounts for the full protection for the metallic iron.

### 3.7 Pilot test

Pilot examinations were also carried out to identify the possible practical troubles. The water quality profiles over the pilot testing period (one month) are illustrated in Fig.7. Under the specified condition, the corrosion rates of C-steel coupons in the presence of ECOSW and CPSW were 0.065 and 0.11 MPY, respectively. This result corresponds to the conclusion from laboratory tests in that the ECOSW is superior to CPSW in corrosion inhibition of C-steel and copper. No serious corrosion spot was observed on the test coupons (including C-steel and Cu coupons) in the presence of either ECOSW or CPSW after pilot test. It is interesting to note that the color of the C-steel surface in the presence of ECOSW turned to light greenish which is likely attributable to the chelation complexa-

tion between gluconate and $Fe^{2+}$. This conclusion is supported by XPS analysis (Fig.5a) in that in the case of ECOSW $Fe^{2+}$ is dominant in Fe $2p^{2/3}$ spectrum as Fe(II) products are known to be greenish in color[10]. A similar phenomenon was also observed for the copper coupon whose surface color is a little bit darker in the case of ECOSW.

Further support about the excellent inhibition capability of ECOSW is also available in that the concentrations of T-Fe in the presence of ECOSW and CPSW after pilot tests were 0.11 and 0.32 ppm, respectively (Fig.7d). On the other hand, the microbial populations over one month span for ECOSW and CPSW were $< 10^2$ and $1.4 \times 10^3$, respectively (Fig.7e). The population of microorganism in the presence of ECOSW is one order of magnitude higher than that of CPSW. This is a predicted result as ECOSW consists of almost 20 wt% of organic matters which provide a sufficient carbon source for microbial growth. However, the level of microbial population with the participation of ECOSW is still lower than the maximum acceptable level by two-order of magnitude (i.e., $10^5$). In addition, ECOSW shows a higher buffer capability than CPSW which is advantageous to suppress the corrosion (Fig.7f). It was also noted that there was a relatively significant increase in conductivity over the testing period in the case of ECOSW (Fig.7g). This result is likely attributed to a combined effect of additional dosage of alkaline and hardness.

## 4. CONCLUSION

An impressive corrosion inhibition with improving cost-performance ratio was developed for a closed-loop cooling water system. Either laboratory or pilot testing revealed that our corrosion inhibitor offered excellent corrosion inhibiting capabilities for C-steel and copper without any bacterial growth issue. A suggested mechanism was also proposed in that gluconate bridges the iron surface and molybdate/nitrite with which a densely stacked film can be formed to protect the target metal from corrosion. In addition, the corrosion inhibitor exhibits a high temperature tolerance up to 70$^o$C. Broad field applications of our developed corrosion inhibitor for closed-loop cooling water systems are expected in the near future. Through utilizing our tailor-made corrosion inhibition program for closed-loop cooling water systems, we believe that we can maximize the profit in terms of water and energy savings.

## REFERENCE

1. T. H. Choi and S. H. Shim: Corrosion & Prevention, 2000, vol. 108, pp. 1-7.
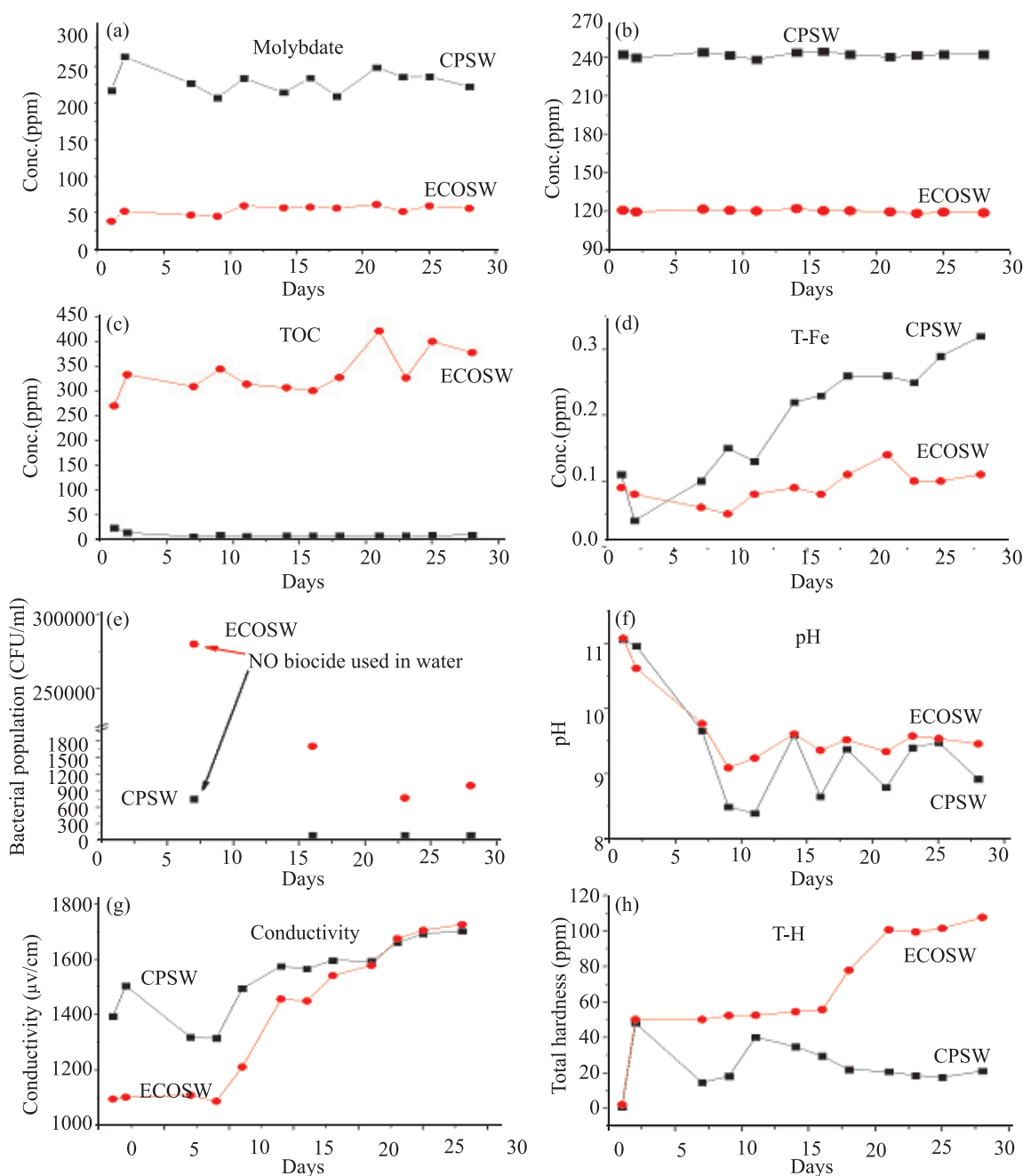2. Y. Y. Thangam M. Kalanithi and C. M. Anbarasi: Arab. J. Sci. Eng., 2009, vol. 34, pp. 51-60.

**Fig.7.** Profile of water quality during one month testing span. (a) Molybdate; (b) Nitrite; (c) Total organic carbon; (d) Total Fe; (e) Bacterial population; (f) pH; (g) Conductivity; and (h) Total hardness.

3. S.M.A. Shibli and V. Anitha Kumary: Anti-Corros Method Mater., 2004, vol. 51, pp.277-281.

4. R. Touir, M. Cenoui, M. El Bakri and M. Ebn Touhami: Corro. Sci., 2008, vol 50, pp. 1530-1537.

5. S. Karim, C. M. Mohammad, M. Asaduzzaman and M. Islam: Leonardo Electronic Journal of Practices and Technologies, 2010, pp. 167-176.

6. S.A.M. Refay: Applied Surface Science, 2000, vol. 157, pp. 199-206.

7. B. S. Maluckov: Metall. Mater. Eng., 2012, vol. 18, pp. 223-231.

8. F. Bentiss, M. Outirite, M. Traisnel, H. Vezin, M. Lagrenee, B. Hammouti, S. S. Al-Deyab and C. Jama: Int. J. Electrochem. Sci., 2012, vol. 7, pp. 1699-1723.

9. Y. Tang, F. Zhang, S. Hu, Cao, Ziyi, Z. Wu and W. Jing: Corro. Sci., 2013, vol. 74, pp. 271-282.

10. D. Ozdemir and V. Cicek : Int. J. Eng. Res. Appl., 2013, vol. 3, PP. 969-985.